

# Evaluation of Selected Rare-Earth Scintillators for Gamma-Ray Sensing Applications

Jasjot Singh Dhillon\* and Yogesh K. Vermani<sup>†</sup>

Department of Physics, Sri Guru Granth Sahib World University, Fatehgarh Sahib-140407, India.

<sup>†</sup>Corresponding author's E-mail: [yugs80@gmail.com](mailto:yugs80@gmail.com)

\*E-mail: [jasjot.jsd@gmail.com](mailto:jasjot.jsd@gmail.com)

## Abstract

In the present work, selected dense rare-earth (RE) based scintillators such as gadolinium tantalate ( $GdTaO_4$ ), gadolinium tantalum-niobates  $Gd(Ta_{0.8}Nb_{0.2})O_4$ , lutetium based  $LuF_3:Ce$ ,  $LuAP:Ce$ ,  $Lu_2O_3:Yb$  and  $Yb_2O_3$  have been investigated for their gamma-ray sensing efficacy. The gamma-ray sensing properties of these RE scintillators have been confronted with modern lead tungstate (PWO) and lead fluoride ( $PbF_2$ ) scintillators being employed recently in high energy physics (HEP) experiments. The attenuation parameters namely linear attenuation coefficient ( $\mu$ ), half value layer (HVL) are compared for these rare-earth scintillators over wide energy range 1keV - 100GeV using Photon Shielding and Dosimetry (PSD) software toolkit. We also attempted to estimate build-up factors (BF's) of these scintillation materials computed using the online platform Py-MLBUF. Our calculations depicted that scintillators containing high-Z rare earth elements exhibited better gamma-ray detection capabilities when compared with standard lead based PWO and  $PbF_2$  scintillators.

## 1. Introduction

Scintillators are the materials which are capable of absorbing the incident photon energy, or particles and corresponding to that energy, scintillators usually emit photons of wavelengths that usually lie in the UV-Vis spectrum. Due to the non-thermal origin of these light photons, these scintillators are also termed 'luminescent' materials. This feature of luminescence assists in the detection of ionizing radiation such as  $\alpha$ -particles,  $\beta$ -particles, X-rays, highly energetic  $\gamma$ -rays, *etc.*

Scintillators have been explored for applications mainly in the medical imaging technology, diagnostic equipment such as digital radiography, PET and SPECT scanners, X-ray computed tomography (CT), *etc.* A highly desirable scintillator material should be able to attenuate the incoming radiation, or



particles and effectively convert the energy absorbed into relatively low-energy photons. The low-energy photon emission corresponds to the bright and sharp pulse spectrum in the detector set-up.

Scintillators bearing high density ( $\rho$ ), and high-Z elements in their elemental compositions are vital for effective photon shielding and stopping power of the absorber material. Moreover, a desirable scintillator also is characterized by larger photon attenuation coefficient, higher light yield (in photons/MeV), and faster decay time  $\tau$  (in ns) [1, 2]. In general, materials with high-Z constituent elements and dense materials demonstrate better radiation attenuation properties as described in our previous work on inorganic scintillators [3, 4], in which lead-based inorganic crystals of PWO and  $\text{PbF}_2$  were shown to have better radiation shielding capabilities against  $\gamma$ -rays. The light yield is also one of the important properties of the scintillation materials measured as the number of emitted photons per MeV of photon energy lost by the incident particles (or, photons) within the absorber medium. In high-energy physics (HEP) experiments, a minimum light yield of  $\sim 250$  photons/MeV is sufficient for the purpose of detection of incident highly energetic particles (and, radiations). The scintillation decay time ( $\tau$ ) is mainly dictated by the time taken by the exciton pairs from the ionization track to reach the emission centers and the lifetime of the luminescence state of the activator. The typical decay time is of the order of nanoseconds (ns) and is directly linked with the timing resolution of the detector incorporating the scintillator. Shorter decay time is an utmost criterion for a scintillator to be used in high counting rate applications such as Mu2e-II experiment, MaRIE at LANL (Los Alamos National Laboratory), TOF detectors and PET *etc*, where best timing resolution is an essential requirement [5, 6, 7].

There exists a class of inorganic scintillators based upon tantalates, tantalum-niobates, fluorides, aluminates, and oxides of several rare-earth (RE) metals (*i.e.*  $\text{La}_{57}$  to  $\text{Lu}_{71}$ ) which exhibit the desirable properties such as high atomic number ( $Z$ ), high density ( $\rho$ ) and high stopping power. Some of these recently developed RE elements based scintillators are listed in **table 1**. The important characteristics of these scintillators include high density values ranging from 8.3 to 9.4  $\text{g/cm}^3$ , higher light yield, and faster decay time. In view of these important features as enlisted in **table 1**, it would be worth interesting to explore these materials for radiation attenuation capabilities. Apart from their shielding efficiency, these scintillators also exhibit faster decay time ( $t$ ) profiles. For instance, the  $\text{GdTa}_{0.8}\text{Nb}_{0.2}\text{O}_4$  scintillator possesses a decay time ( $t$ ) as fast as 12 ns with no slow component [4].  $\text{Lu}_2\text{O}_3:\text{Yb}$  bears an ultrafast decay time of 1.3 ns, while  $\text{Yb}_2\text{O}_3$  exhibits a sub-ns decay time of 0.22 ns which is faster than the standard decay time of 0.5 ns possessed by the ultrafast  $\text{BaF}_2:\text{Y}$  scintillator [6, 8].  $\text{BaF}_2:\text{Y}$  also possesses a slow component suppressed by the optimal doping concentration of Yttrium ions. Gadolinium-based tantalates *i.e.*  $\text{GdTaO}_4$  (GTO) are observed to have a high density of 8.94  $\text{g/cm}^3$  and there have been developments in manufacturing crack-free high-quality crystals [9]. This is the highest density value achieved among the currently employed single crystal scintillators. Further,  $\text{GdTaO}_4$  and  $\text{GdTa}_{0.8}\text{Nb}_{0.2}\text{O}_4$  scintillation materials are also reported to have light yields, respectively, 3 and 13 times that of PWO [4, 9]. It can be inferred that PWO may not be bright enough for most applications as the light yield of PWO is only 250 photons/MeV. In experiments related to high-energy physics calorimeters, advanced RE based scintillators can offer higher stopping power in combination with adequate light yield and short decay time. [10]. In view of these peculiar features, it is worthwhile to investigate these high density scintillators for photon attenuation properties and

confront the observations with those of currently employed high density PWO scintillators. This knowledge is of paramount importance to select the best scintillation material for faster and more effective radiation detection. An optimal scintillator with a combination of high density, enhanced light output and shorter decay time ( $t$ ) is LuAP ( $\text{LuAlO}_3$ ). Lutetium Fluoride ( $\text{LuF}_3$ ) is another very useful RE-based scintillator that displays scintillation spectrum in the vacuum ultraviolet (VUV) region.  $\text{LuF}_3$  is widely employed in micro-pattern gaseous detectors (MPGDs). Moreover, these materials are cost-effective and promising crystals for large area detection applications with competent spatial resolution [11, 12].

In the present research work, we shall aim to compute the photon attenuation parameters namely linear attenuation coefficient (LAC) and half value layer (HVL) values using Phy-X/PSD online software [13] over broad energy range from 1 keV to 100 GeV. We shall also attempt calculating buildup factors (BF's) of investigated scintillators using the recently developed software toolkit namely 'py-MLBUF' [14].

## 2. Methodology

The Interaction mechanism of incident radiations (or, particle) with absorber /detector material depends upon the incident energy of photon/particle. For instance, low energy and extremely high energy gamma-ray photons are completely absorbed (*i.e.* via photoelectric effect and pair production phenomena, respectively). Interaction of photons having intermediate energy leads to Compton and Rayleigh scattering phenomena. These interaction processes bear respective interaction cross-sections measuring the likelihood of these phenomena. The interaction cross-sections depend upon the incident energy of the gamma-rays as well as the composition of sensing material. If the gamma radiation is a mono-energetic, narrow beam and the material layer in question (*i.e.* sensing material) is thin, then the attenuated intensity after passing through the material layer is given by the following equation:

$$I = I_0 e^{-\mu x}. \quad \text{Eq. (1)}$$

Here,  $I_0$  is the intensity of incident gamma-radiation, ' $x$ ' is the thickness of the material (in centimeters), and  $\mu$  is the linear attenuation coefficient (in  $\text{cm}^{-1}$ ). This equation is the well-known Lambert-Beer law [13] which is applicable only if the above-mentioned conditions are satisfied. If the experimental narrow beam transmission setup fails to meet any of these requirements, the deviation from the Intensity equation Eq. (1) is adjusted by inserting a multiplicative factor  $B$ . This corrective factor is known as the build-up factor (BUF). The build-up factor (BUF) takes into account the multiple-scattering of gamma-ray photons within the absorber material. The minimum value for BF is 1 indicating that conditions for narrow beam transmission through a thin layer of sensing material are satisfied. The corrected intensity equation (or, Lambert-Beer law) takes the form:

$$I = B I_0 e^{-\mu x} \quad \text{Eq. (2)}$$

The linear attenuation coefficient  $\mu$  is usually obtained from mass attenuation coefficient (MAC) denoted by  $\mu_m$ . This parameter is a measure of the probability of interaction of the incident radiation/particle with per unit mass of the absorber and encompasses the total attenuation. It is usually measured in units of  $\text{cm}^2/\text{g}$ . For a material composed of different elements, it is determined using the mixture rule given by Jackson and Hawkes [15]:

$$\mu_m = \frac{\mu}{\rho} = \sum_i w_i (\mu_m)_i. \quad \text{Eq. (3)}$$

**Table 1.** Elemental composition, density, and other important properties of rare-earth-based scintillation materials.

Rare-earth scintillators	Elemental composition (wt.%)	Light yield (photons/MeV)	Decay time, $\tau$ (ns)	Density, $\rho$ (g/cm <sup>3</sup> )	Ref.(s)
<b>GdTaO<sub>4</sub></b>	40.0948 % Gd 43.5874 % Ta 16.3178 % O	~ 750	72.6, 1236.2	8.94	[4, 9, 16]
<b>GdTa<sub>0.8</sub>Nb<sub>0.2</sub>O<sub>4</sub></b>	41.7566 % Gd 36.3152 % Ta 4.9341 % Nb 16.994 % O	~ 3250	12	8.37	[4]
<b>LuF<sub>3</sub>: Ce (0.04 at %)</b>	75.4109 % Lu 24.5640 % F 0.0242 % Ce	8000	23	8.3	[17, 18, 19]
<b>LuAlO<sub>3</sub>: Ce (0.11 wt. %)</b>	72.2317 % Lu 7.8431 % Al 19.8150 % O 0.1100 % Ce	21000	18	8.34	[11, 20]
<b>Lu<sub>2</sub>O<sub>3</sub>: Yb (0.3% atoms of Lu replaced by Yb)</b>	87.7086 % Lu 12.0304 % O 0.2610 % Yb	500	1.3	9.4	[8, 21, 22]
<b>Yb<sub>2</sub>O<sub>3</sub></b>	87.8201 % Yb 12.1799 % O	-	0.22	9.2	[21, 22, 23]
<b>PWO</b>	45.5337 % Pb 40.4023 % W 14.0640 % O	~ 250	5-15	8.28	[2, 24]
<b>PbF<sub>2</sub></b>	84.5038 % Pb 15.4962 % F	< 1000	30, 6	7.77	[25, 26]

Here,  $w_i$  is the weight fraction and  $(\mu_m)_i$  is the mass attenuation coefficient of the  $i$ th element present in the mixture. The next important sensing parameter is half-value layer (HVL). It is defined as the thickness of the absorber material (or, scintillator in present work) that attenuates the intensity of incident radiation to half of its original value. It is obtained from the linear attenuation coefficient  $\mu$  using the relation [13]:

$$HVL = \frac{0.693}{\mu} \quad \text{Eq. (4)}$$

The build-up factor (BUF) is of two types: Energy Absorption Build-up Factor (EABF) and Exposure Build-up Factor (EBF). EABF is related to photon energy deposition within the scintillator medium, while EBF deals with the exposure and absorption in the air. Theoretically, these build-up factors are evaluated for different thickness layers of the scintillator material and over wide incident energy from 0.015 MeV to 15 MeV. We shall evaluate exposure build-up factor (EBF) as functions of photon energy range and different penetration depths (in mfp) using the online toolkit 'py-MLBUF'.

### 3. Analysis and Discussion

The linear attenuation coefficient (LAC) is the sum of interaction cross-sections for all absorption and scattering modes. Relative cross-sections for these different modes of interaction are dependent on the

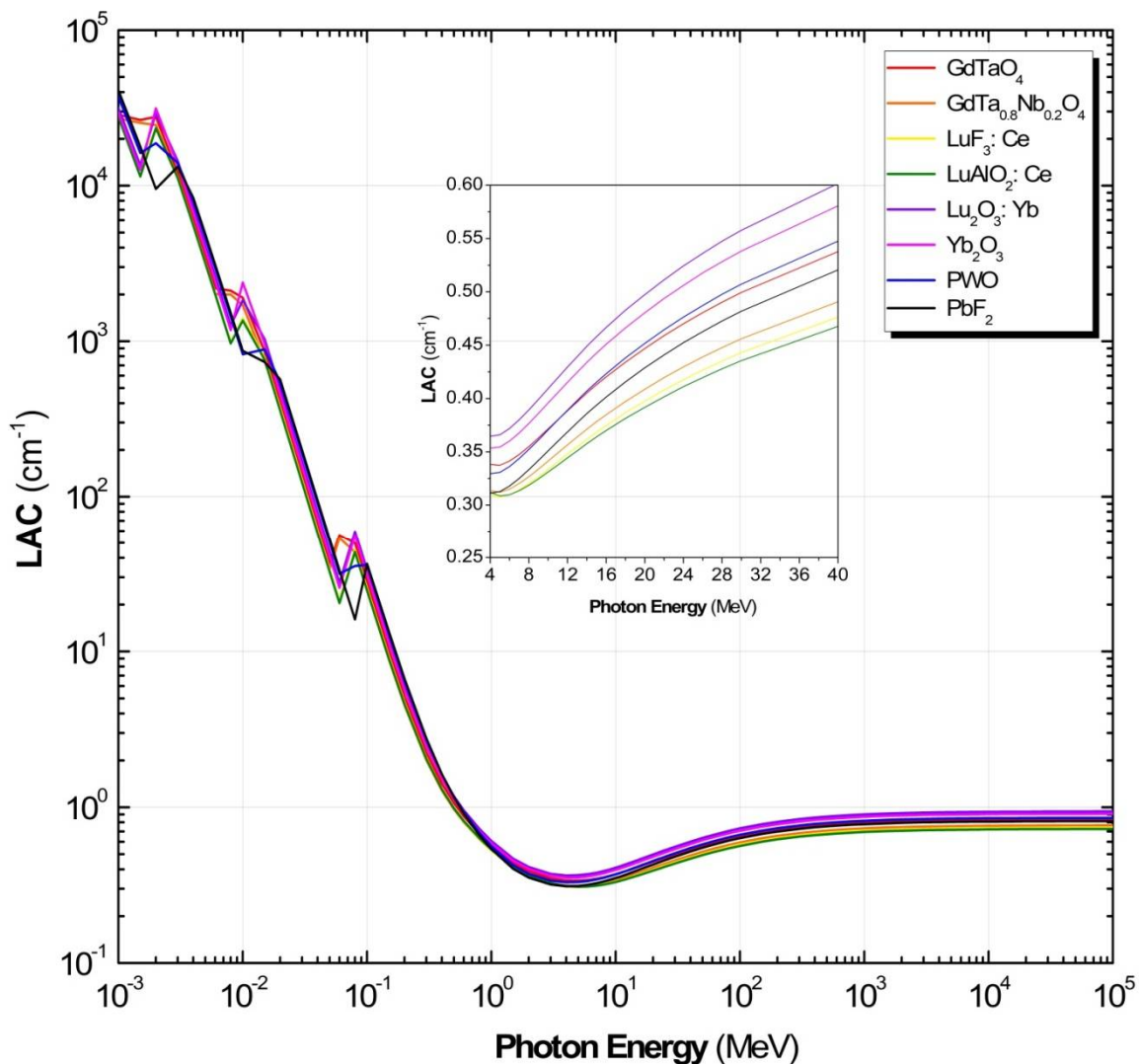


**Fig 1.** Linear attenuation coefficient (LAC) computed as function of gamma-ray energy for various inorganic high-Z scintillators using online *Photon Shielding and Dosimetry* (PSD/Phy-X) software tool. Inset of Fig. 1 shows the magnified view of LAC vs photon energy curves.

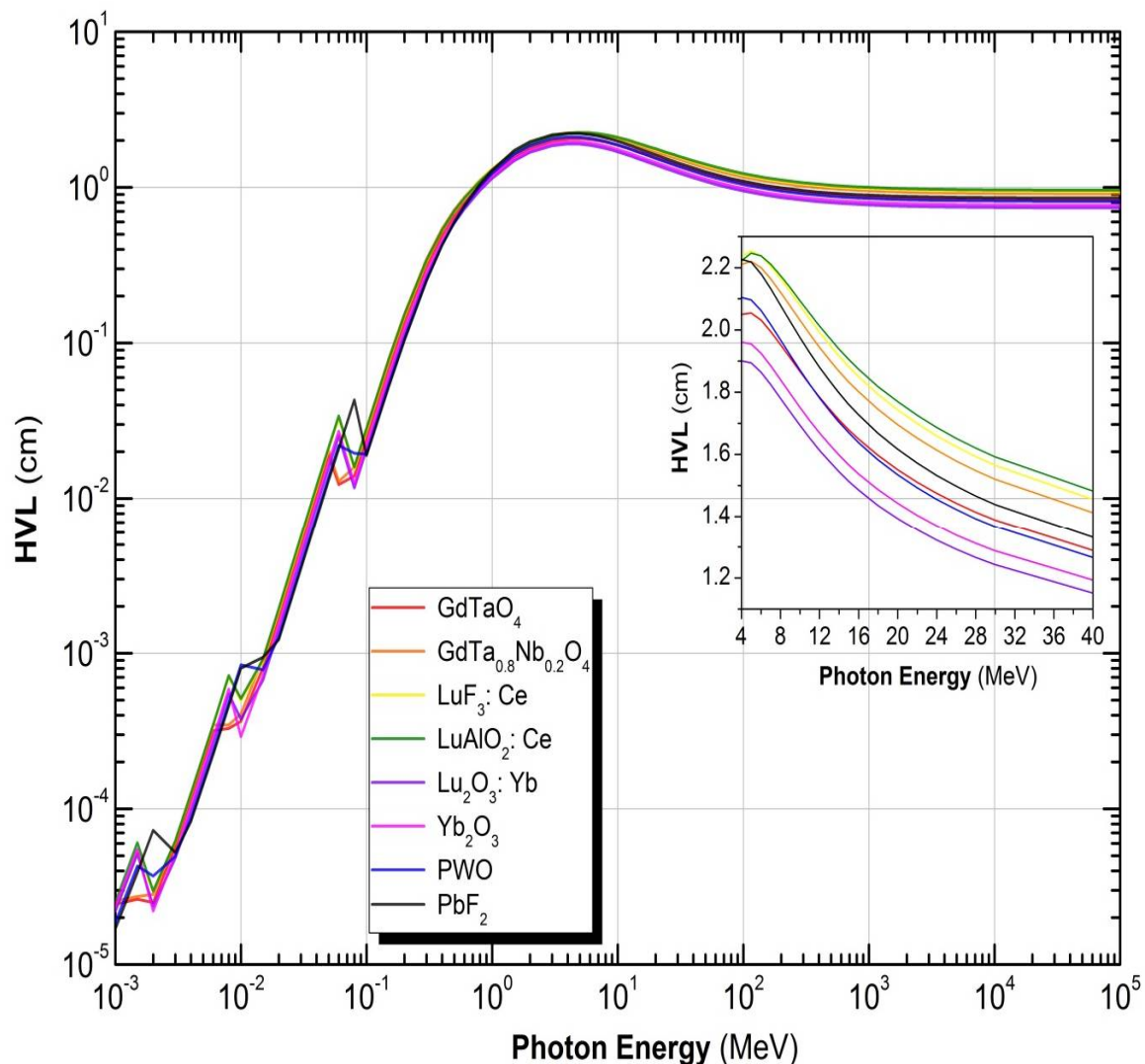


**Fig 2.** Variation of half value layer (HVL) *w.r.t.* gamma-ray photon energy in the range 1 keV-100 GeV computed using online *Photon Shielding and Dosimetry (PSD/Phy-X)* software tool. Inset of Fig. 2 shows the magnified view of HVL vs photon energy curves for  $E_\gamma > 4$  MeV.

absorber material (inorganic scintillators, in present case) properties such as density, atomic number  $Z$  of the constituent elements, and the energy of the incident gamma radiation.

In **Fig. 1**, we display linear attenuation coefficient (LAC) computed for selected inorganic scintillators as function of photon energy  $E_\gamma$ . Below photon energy 500 keV, all scintillation materials possess higher values of LAC. The linear attenuation coefficient values decrease as we go towards higher photon energies, this is because the dominant photo-electric absorption process for which interaction the cross section varies as  $\sigma_{PE} \propto Z^{4-5}/E^{3.5}$  [27, 28, 29]. As clear from the Fig. 1, better radiation attenuation capability is displayed by rare earth (RE) based scintillators namely  $\text{Lu}_2\text{O}_3:\text{Yb}$  and  $\text{Yb}_2\text{O}_3$  which is further comparable with those of high density lead based PWO and  $\text{PbF}_2$  scintillators. PWO and  $\text{PbF}_2$  scintillators are best sensing materials at lower energies owing to their high  $Z$  constituent elements

and higher density values. There are observed sharp spikes in the LAC versus photon energy curves particularly in lower energy regime owing to the occurrence of absorption edges. In the intermediate energy regime upto 3 MeV, dominant interaction mode is Compton scattering of incident gamma-ray photons for which interaction cross-section moderately dependent on  $Z$  and the incident photon energy [27]. As a result, the attenuation behavior by all scintillators in this energy regime follows a similar trend and  $\text{Lu}_2\text{O}_3:\text{Yb}$  and  $\text{Yb}_2\text{O}_3$  scintillators exhibit the highest values of LAC. For higher photon energies  $E_\gamma > 3$  MeV, linear attenuation coefficient increases gradually again. In this energy regime, complete photon absorption occurs via pair production phenomenon for which interaction cross-section varies as  $\sigma_{pp} \propto Z^2 \cdot \log E_\gamma$  [27, 29]. Since most of the inorganic scintillators are to be used for detection applications in the high energy radiation environment, so we are more concerned with investigation of nuclear absorption characteristics of high- $Z$  rare earth based scintillators in high-energy regime.

Next we evaluate the half value layer (HVL) as function of photon energy using user friendly *Photon Shielding and Dosimetry (PSD) software tool* [13]. HVL being inversely proportional to the first power of LAC, thus displays a reverse trend for HVL versus photon energy curves as displayed in **Fig. 2**. In other words, HVL values are found to increase sharply with photon energy. In the lower energy region, high- $Z$  Pb based scintillators  $\text{PbF}_2$  and PWO exhibit the least HVL values. In the intermediate and higher energy regions, however, rare earth based  $\text{Lu}_2\text{O}_3:\text{Yb}$  and  $\text{Yb}_2\text{O}_3$  scintillators offer better gamma-ray sensing capabilities. This is clearly evident from lowest HVL values as illustrated in inset of **Fig. 2**. At higher photon energies ( $\geq 100$  MeV), HVL values almost saturate for all materials with minimum value registered for  $\text{Lu}_2\text{O}_3:\text{Yb}$  (0.89 cm) and  $\text{Yb}_2\text{O}_3$  (.92 cm), while lead based PWO and  $\text{PbF}_2$  display relatively higher values of 0.98 cm and 1.03 cm, respectively at 150 MeV photon energy. This comparative analysis of HVL values gives an idea about the extent to which thickness of scintillation detector material can be reduced by using the material with lowered half value layer values in high-energy radiation environment.

In case the thickness of the absorber material is not sufficiently low, there would be enhanced production of secondary photons attributing to higher photon build-up factor (BUF) values. Meanwhile, the scattering phenomena such as Compton scattering of photons directly contributes to the photon build-up and thereby increase in exposure buildup factor (EBF) value. The variation of EBF with gamma-ray energy for investigated inorganic scintillators is shown in **Figs. 3(a) and 3(b)** at penetration depths of 1 mfp and 20 mfp, respectively. The EBF values are close to unity ( $\approx 1$ ) for lower incident photon energies (below 30 keV) owing to complete removal of photons via photoelectric absorption process. In the energy range between 0.03 MeV to 0.15 MeV, the build-up factor values attain peak values are maximum as evident via peaks in curves corresponding to different scintillator materials. These peaks are commonly attributed to the absorption edges of the different constituent elements present in scintillation detector materials. In photon energy range 0.08 - 0.2 MeV,  $\text{LuAlO}_3:\text{Ce}$  (Lutetium aluminum perovskite) and  $\text{Gd}(\text{Ta}_{0.8}\text{Nb}_{0.2})\text{O}_4$  exhibit minimal EBF values. In the intermediate and high energy domain 0.2 - 3 MeV, the Compton scattering of gamma photons and pair production are the dominant processes, respectively. Compton scattering of incident is the major contributor for multiple scattering events and rise of secondary gamma-ray photons. In pair production domain, photons are absorbed again and there is rise in multiple scattering events [30, 31]. Thus, we observe a steady increase in the EBF values in the intermediate energy regime. For 20 mfp penetration depth, EBF values

obtained were higher, while these were lowest at 1 mfp. In other words, deviation from the Beer-Lambert law is the least for 1 mfp penetration depth. Interestingly, rare-earth elements based scintillators  $\text{Lu}_2\text{O}_3:\text{Yb}$  and  $\text{Yb}_2\text{O}_3$  exhibit minimal EBF values as compared to other RE based inorganic scintillators which are further comparable with those of lead containing  $\text{PbF}_2$  and  $\text{PbWO}$  scintillators in the intermediate energy domain. After 3 MeV photon energy, pair production is the most probable interaction mode with scintillation detector material. Electron-positron pair thus created may further interact with host material and will result in release of electromagnetic radiation after annihilation. The EBF values of these materials would further rise again with photon energy. After 6 MeV, the build-up factor increases with further increase in energy and saturate to similar values for all scintillation materials at higher photon energies as shown in **Fig. 3**.

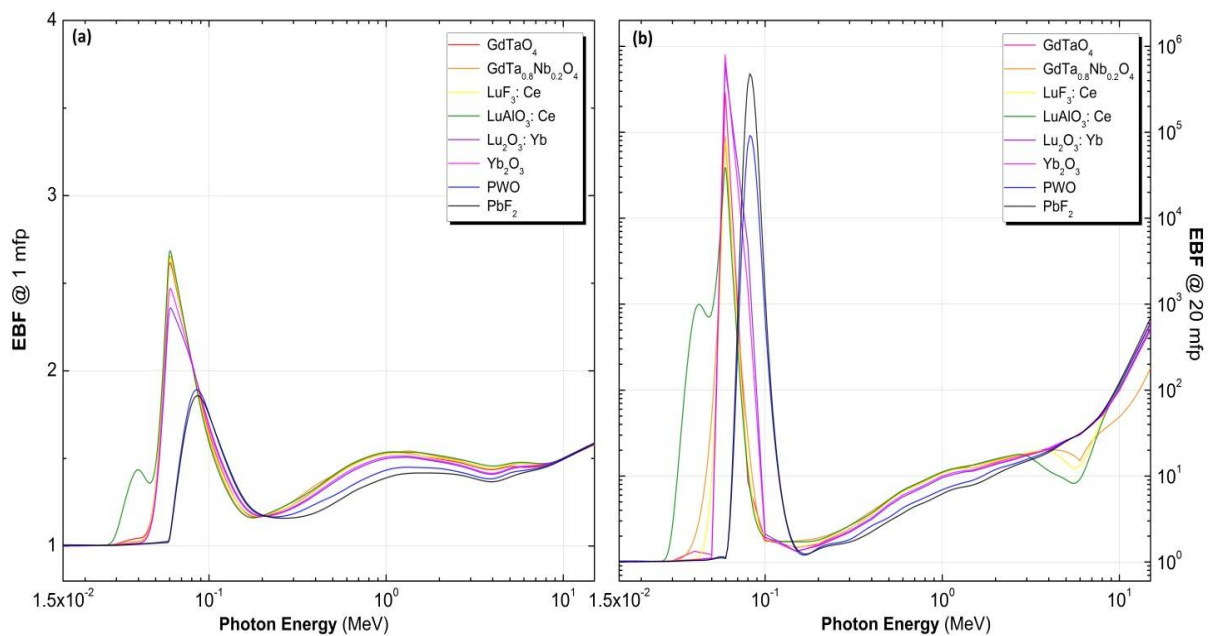


**Fig 3.** Exposure build-up factor (EBF) versus gamma-ray energy curves plotted at (a) 1 mfp and (b) 20 mfp penetration depths.

#### 4. Conclusions

Present analysis investigates radiation shielding and sensing characteristics of selected dense rare-earth and lead containing scintillators across wide range of incident photon energies. In particular, lead based PWO and  $\text{PbF}_2$  scintillators are found to bear higher LAC and lower HVL values in lower energy regime. That is, highly dense and high-Z lead based scintillators offers better attenuation against gamma radiations at lower photon energies. For higher energy regime, however, high density rare-earth containing  $\text{Lu}_2\text{O}_3:\text{Yb}$  and  $\text{Yb}_2\text{O}_3$  scintillators exhibit highest LAC values and consequently, lowest HVL values. In view of the fact that  $\text{Lu}_{71}$  and  $\text{Yb}_{70}$  based scintillators require lesser thickness layer as compared to Pb-based scintillators, these RE based materials can prove to prospective candidates for development of scintillators operating in high energy domains. Variation of EBF values with photon energy analyzed at penetration depths of 1 mfp and 20 mfp indicated significant influence of elemental

composition, density and gamma-ray energy incident. One can infer from this comparative analysis that RE based  $\text{Lu}_2\text{O}_3:\text{Yb}$  and  $\text{Yb}_2\text{O}_3$  scintillators are superior candidates for gamma-ray attenuation and sensing applications in high energy physics experiments.

## References

- [1] Yanagida T 2018 "Inorganic scintillating materials and scintillation detectors" *Proc. Jpn. Acad., Ser. B* **94** 75-97
- [2] Moses William W 2002 "Current trends in scintillator detectors and materials" *Nucl. Instrum. Methods Phys. Res. A* **487** 123-128
- [3] Dhillon J S and Vermani Y K 2022 "Gamma-Ray Interaction of Selected Inorganic Scintillators Used in HEP Experiments" *IOP Conf. Ser.: Mater. Sci. Eng.* **1221** 012002
- [4] Voloshyna OV *et al* 2014 "New, dense, and fast scintillators based on rare-earth tantalate-niobates" *Nucl. Instrum. Methods Phys. Res. A* **764** 227-231
- [5] Zhu Ren-Yuan 2019 "Ultrafast and radiation hard inorganic scintillators for future HEP experiments" *J. Phys. Conf. Ser.* **1162** 012022
- [6] Hu Chen *et al* 2019 "Development of yttrium-doped  $\text{BaF}_2$  crystals for future HEP experiments" *IEEE Trans. Nucl. Sci* **66** 1854-1860
- [7] Hu Chen *et al* 2019 "Ultrafast inorganic scintillator-based front imager for Gigahertz Hard X-ray imaging" *Nucl. Instrum. Methods Phys. Res. A* **940** 223-229
- [8] Yanagida T *et al* 2014 "Optical and scintillation properties of transparent ceramic  $\text{Yb}:\text{Lu}_2\text{O}_3$  with different Yb concentrations" *Opt. Mater* **36** 1044-1048
- [9] Yang Huajun *et al* 2014 "A promising high-density scintillator of  $\text{GdTaO}_4$  single crystal" *Cryst Eng Comm* **16** (12) 2480-2485
- [10] Weber MJ *et al* 1995 "Dense  $\text{Ce}^{3+}$ -activated scintillator materials" *Proceedings of SCINT, Delft, The Netherlands* Vol. **95**
- [11] Zych E *et al* 1998 "Infrared spectroscopy of  $\text{LuAlO}_3:\text{Ce}$  a useful tool to determine Ce concentration." *Spectrochim. Acta A: Mol. Biomol. Spectrosc* **54** 1763-1769
- [12] Fukuda Kentaro *et al* 2011 "Crystal growth and optical properties of the  $\text{Nd}^{3+}$  doped  $\text{LuF}_3$  single crystals" *Opt. Mater* **33** 1143-1146
- [13] Şakar Erdem *et al* 2020 "Phy-X/PSD: development of a user friendly online software for calculation of parameters relevant to radiation shielding and dosimetry" *Radiat. Phys. Chem.* **166** 108496
- [14] Mann K S and Maan S S 2021 "Py-MLBUF: Development of an online-platform for gamma-ray shielding calculations and investigations" *Ann. Nucl. Energy* **150** 107845
- [15] Jackson Daphne F and David J Hawkes 1981 "X-ray attenuation coefficients of elements and mixtures" *Phys. Rep.* **70** 169-233
- [16] Dou Renqin *et al* 2018 "Rare-earth tantalates and niobates single crystals: Promising scintillators and laser materials" *Crystals* **8**(2) 55
- [17] Moine Bernard *et al* 1997 "Spectroscopic and scintillation properties of cerium-doped  $\text{LuF}_3$  single crystal" *Materials Science Forum* **239** Trans Tech Publications Ltd 245-248

- [18] Birowosuto M D and P Dorenbos 2009 "Novel  $\gamma$ - and X-ray scintillator research: On the emission wavelength, light yield and time response of  $\text{Ce}^{3+}$  doped halide scintillators" *Phys. Status Solidi A* **206** 9-20
- [19] Guerbous L and Krachni O 2006 "The 4f-5d luminescence transitions in cerium-doped  $\text{LuF}_3$ " *J. Mod. Opt.* **53** 2043-2053
- [20] Bartram R H *et al* 1997 "Electron traps and transfer efficiency of cerium-doped aluminate scintillators" *J. Lumin.* **75** (3) 183-192
- [21] Fukabori Akihiro *et al* 2011 "Growth of  $\text{Y}_2\text{O}_3$ ,  $\text{Sc}_2\text{O}_3$  and  $\text{Lu}_2\text{O}_3$  crystals by the micro-pulling-down method and their optical and scintillation characteristics" *J. Cryst. Growth* **318** 823-827
- [22] Yanagida T *et al* 2011 "Ultrafast Transparent Ceramic Scintillators Using the  $\text{Yb}^{3+}$  Charge Transfer Luminescence in  $\text{RE}_2\text{O}_3$  Host" *Appl. Phys. Express* **4** 126402
- [23] Derenzo Stephen E *et al* 1990 "Prospects for new inorganic scintillators" *IEEE Trans. Nucl. Sci* **37** 203-208
- [24] Lecoq P *et al* 1995 "Lead tungstate ( $\text{PbWO}_4$ ) scintillators for LHC EM calorimetry" *Nucl. Instrum. Methods Phys. Res. A* **365** 291-298
- [25] Anderson D F *et al* 1990 "Lead fluoride: An ultra-compact Cherenkov radiator for EM calorimetry" *Nucl. Instrum. Methods Phys. Res. A* **290** 385-389
- [26] Mao Rihua *et al* 2012 "Crystals for the HHCAL detector concept" *J. Phys. Conf. Ser.* **404** 012029
- [27] Singh T *et al* 2018 "Gamma rays' shielding parameters for some Pb-Cu binary alloys" *Eng. Sci. Technol.* **21**(5) 1078-1085
- [28] Kilicoglu O and Tekin H O 2020 "Bioactive glasses and direct effect of increased  $\text{K}_2\text{O}$  additive for nuclear shielding performance: A comparative investigation" *Ceram. Int.* **46**(2) 1323-1333
- [29] Kaur T *et al* 2017 "Feasibility of Pb-Zn binary alloys as gamma rays shielding materials" *Int. J. Pure Appl. Phys.* **13**(1) 222-225
- [30] Singh V P *et al* 2014 "Study on  $\gamma$ -ray exposure buildup factors and fast neutron-shielding Properties of some building materials" *Radiat. Eff. Defects Solids* **169**(6) 547-559
- [31] Al-Buriahi M S and Tonguc B T 2019 "Study on gamma-ray buildup factors of bismuth borate glasses" *Appl. Phys. A* **125** (7) 1-7